Polymerization Hot Paper

How to cite:
International Edition: doi.org/10.1002/anie.202114896
German Edition: doi.org/10.1002/ange.202114896

Inverse Vulcanization of Norbornenylsilanes: Soluble Polymers with Controllable Molecular Properties via Siloxane Bonds

Johannes M. Scheiger, Maxi Hoffmann, Patricia Falkenstein, Zhenwu Wang, Mark Rutschmann, Valentin W. Scheiger, Alexander Grimm, Klara Urbschat, Tobias Sengpiel, Jörg Matysik, Manfred Wilhelm, Pavel A. Levkin, and Patrick Theato**

Abstract: *The inverse vulcanization produces high sulfur content polymers from alkenes and elemental sulfur. Control over properties such as the molar mass or the solubility of polymers is not well established, and existing strategies lack predictability or require large variations of the composition. Systematic design principles are sought to allow for a targeted design of materials. Herein, we report on the inverse vulcanization of norbornenylsilanes (NBS), with a different number of hydrolysable groups at the silicon atom. Inverse vulcanization of mixtures of NBS followed by polycondensation yielded soluble high sulfur content copolymers (50 wt% S) with controllable weight average molar mass (M_W), polydispersity (Đ), glass transition temperature (T_G), or zero-shear viscosity (η_0). Polycondensation was conducted in the melt with HCl as a catalyst, abolishing the need for a solvent. Purification by precipitation afforded polymers with a greatly reduced amount of low molar mass species.*

Introduction

The desulfurization of natural oil and gas is an essential process prior to the use of fossil fuels. Therefore, residual sulfur is available on the megaton scale. For ecological and environmental reasons, surplus produced sulfur should be treated as a resource rather than as a waste material. The inverse vulcanization reported in 2013 opened a path to convert elemental sulfur into polymers,[1] which have later been employed for a wide range of applications such as the remediation of mercury, perfluorooctanoic acid, or hydrocarbon spills,[2] anti-microbial surfaces,[3] adhesives,[4] metal and particle templates,[5] infrared optics,[6] cathode materials,[7] healable or recyclable materials,[8] thermal insulators,[9] flame retardants,[10,11] or fertilizers.[12] The literature accounts for different naming styles of products obtained by inverse vulcanization, such as sulfur copolymers, inverse vulcanized polymers, Ormochalks, or CHIPS. While the term vulcanization according to IUPAC refers to the chemical crosslinking to give a polymer network, it has not been clearly defined for inverse vulcanization if inverse accounts only for the composition or also its structure.[13] Hence, in the following we will refer to all products obtained by inverse vulcanization as inverse vulcanized polymers regardless of their solubility, i.e., their structure. Inverse vulcanizations are typically conducted by heating elemental sulfur together with suitable alkenes to 130–180 °C, resulting in sulfur copolymers with a sulfur content varying from 20–90 wt %.[14] The range of polymerizable vinyl compounds was greatly extended by the development and study of catalytic inverse vulcanizations by Hasell and Pyun.[15] In contrast to the well-established polymer chemistry of carbon, controlling fundamental parameters of inverse vulcanized polymers, such as the molar mass, the solubility, or the thermomechanical properties, is challenging and

[*] J. M. Scheiger, Z. Wang, Prof. P. A. Levkin
Institute of Biological and Chemical Systems–Functional Molecular Systems (IBCS-FMS), Karlsruhe Institute of Technology (KIT)
Hermann-von-Helmholtz-Platz 1, 76344
Eggenstein-Leopoldshafen (Germany)
E-mail: levkin@kit.edu

J. M. Scheiger, M. Hoffmann, A. Grimm, K. Urbschat, T. Sengpiel, Prof. M. Wilhelm, Prof. P. Theato
Institute for Technical Chemistry and Polymer Chemistry (ITCP)
Karlsruhe Institute of Technology (KIT)
Engesserstrasse 18, 76131 Karlsruhe (Germany)
E-mail: patrick.theato@kit.edu

P. Falkenstein, Prof. J. Matysik
Leipzig University, Institute of Analytical Chemistry
Linnéstrasse 3, 04103 Leipzig (Germany)

M. Rutschmann
Institute of Inorganic Chemistry (IAC), Karlsruhe Institute of Technology (KIT)
Engesserstrasse 15, 76131 Karlsruhe (Germany)

V. W. Scheiger
Institute of Applied Informatics and Formal Description Methods (AIFB), Karlsruhe Institute of Technology (KIT), Kaiserstrasse 89
76133 Karlsruhe (Germany)

Prof. P. A. Levkin
Institute for Organic Chemistry, Karlsruhe Institute of Technology (KIT)
Fritz-Haber-Weg 6, 76313 Eggenstein-Leopoldshafen (Germany)

Prof. P. Theato
Soft Matter Synthesis Laboratory - Institute for Biological Interfaces III (IBG-3), Karlsruhe Institute of Technology (KIT)
Hermann-von-Helmholtz-Platz 1, 76344 Eggenstein-Leopoldshafen (Germany)

depends strongly on the reaction conditions.[16] Initially, the feed ratio of sulfur was used as the main variation parameter to influence the properties of inverse vulcanized polymers, which showed to be insufficient to address a wide range of properties. Hasell and co-workers developed ternary inverse vulcanizations, which induced control over the physical properties by means of the relative ratio of different alkenes or by employing alkenes with different reactivity to enable delayed curing.[17,18] However, the influence of an alkene on the properties of an inverse vulcanized polymer are hard to predict. The most recent strategy to prepare polymers with tailored mechanical properties is the inverse vulcanization of post-curable moieties followed by a post-curing step. Based on the reaction of alcohols with isocyanates to form urethane crosslinks, Hasell and Pyun demonstrated inverse vulcanized polymers with the most intriguing mechanical properties reported so far, i.e., a high strength and elasticity.[10,18] Achieving both a high stress (>10 MPa) and elongation strain (>300 %), however, required a reduction of the sulfur content to only 20 wt %.[19] Further, the procedure required a complex mixture of 10-undecen-1-ol, methylendiphenylisocyanate, 1,4-butanediol, vinyl capped polydimethylsiloxane or diisopropenylbenzene, and *N*,*N*′-dimethylformamide as a solvent. So far, the partial crosslinking of alcohols with isocyanates to obtain urethanes has been the only reported post-curing strategy compatible with the inverse vulcanization to produce thermosets and thermoplastics with tunable properties. Thus, a diversification of post-curing strategies is highly desirable.

Previously, we reported on the inverse vulcanization, hydrolysis and polycondensation of styrylethyltrimethoxysilane to obtain room-temperature curable high sulfur content coatings.[20] However, the polycondensation of trialkoxysilanes results in crosslinked and insoluble siloxane networks, which is thus not a suitable strategy to prepare soluble polymers. We hypothesized, that hydrolysable silanes can be used to control the molecular properties of inverse vulcanized polymers, when the average number of hydrolysable groups per silane is far below that of a trialkoxysilane. A lower number of hydrolysable groups should lead to fewer siloxane bonds between inverse vulcanized polymers and generate soluble, branched polymers. Introducing predictable chemical variation parameters into the still largely unpredictable inverse vulcanization is required to establish systematic design principles for the preparation of high sulfur content materials with defined molecular or mechanical properties. Herein, we report the inverse vulcanization of norbornenylsilanes for the controlled and targeted preparation of high sulfur content polymers. Norbornenylsilanes (NBS, not to be confused with *N*-bromosuccinimide) carry C=C double bonds that are known to react with sulfur at elevated temperatures.[18] The chosen NBS contain a different number of hydrolysable chloro- or ethoxy substituents, allowing them to form M, D, or T siloxane bonds upon polycondensation. Control over the properties of high sulfur content polymers is achieved by mixing different NBS before reacting them with sulfur. The sulfur content can be kept the same, while the properties of the polymers are altered significantly. Importantly, NBS can be produced from commodity chemicals that are available on an industrial scale (vinyltrialkoxysilanes and cyclopentadiene, or norbornadiene and trichlorosilane), rendering the strategy proposed herein scalable.

Results and Discussion

Inverse vulcanization reactions of sulfur as monomer, the non-hydrolysable trimethylnorbornenylsilane (TMNBS) as a comonomer, and a hydrolysable norbornenylsilane (NBS) as a termonomer were conducted using different ratios of norbornenylsilanes. The mixture of TMNBS with a hydrolysable NBS is denoted as NBS_x, in which NBS refers to the name of the hydrolysable NBS (i.e., MENBS, DENBS, TENBS, DCNBS, or TCNBS) and the index *x* refers to the weight percentage (wt %) of the hydrolysable NBS relative to the total mass of NBS_x. Equal masses of sulfur and NBS_x were reacted at 150 °C for 5 h to obtain polymers of the general formula poly(S-*r*-NBS_x). Melt polycondensation of poly(S-*r*-NBS_x) resulted in the formation of soluble *branch*-poly(S-*r*-NBS_x) polymers with controllable molecular and macroscopic properties, depending on the exact composition of the NBS mixture (Scheme 1A). This is due to the presence of either M, D, or T siloxane binding motifs in the *branch*-poly(S-*r*-NBS_x) polymers (Scheme 1B). A brief sum-

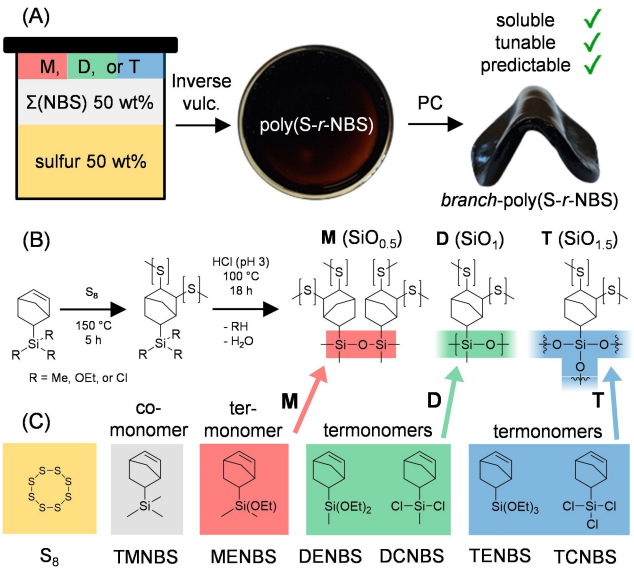

Scheme 1. A) Schematic reaction equation of the inverse vulcanization of sulfur with a mixture of norbornenylsilanes (NBS_x), followed by polycondensation (PC). A mixture of NBS containing either a M, D, or T siloxane precursor reacts with sulfur to form poly(S-*r*-NBS_x), which is polycondensated to form *branch*-poly(S-*r*-NBS_x). B) General reaction equation of the inverse vulcanization of sulfur with a mixture of norbornenylsilanes (NBS), followed by polycondensation. Depending on the NBS used, the *branch*-poly(S-*r*-NBS_x) polymer contains either M, D, or T siloxane bonds. C) Chemical structures, acronyms, and color code of NBS serving as comonomer (TMNBS) or as termonomer to generate M siloxane (MENBS), D siloxane (DENBS, DCNBS), or T siloxane (TENBS, TCNBS) bonds.

mary about the polycondensation and nomenclature of silanes is provided in the Supporting Information (Figure S1). A typical NBS_x mixture consisted of 90–50 wt % of TMNBS and 10–50 wt % of a hydrolysable NBS. As hydrolysable NBS, the M siloxane precursor monoethoxynorbornenylsilane (MENBS), the D siloxane precursors diethoxynorbornenylsilane (DENBS) and dichloronorbornenylsilane (DCNBS), or the T siloxane precursors triethoxynorbornenylsilane (TENBS) and trichloronorbornenylsilane (TCNBS) were used (Scheme 1C).

Importantly, the hydrolysable groups remain unaffected by the harsh conditions of the inverse vulcanization (Figure S2). Trimethylnorbornenylsilane (TMNBS) was synthesized from the reaction of MENBS with MeLi and was characterized with ATR FT-IR, ^{1}H, ^{13}C, and ^{29}Si NMR spectroscopy (Figure S3–S5).

To ensure that the reaction of NBS_x with sulfur does not lead to sole consumption of just one of the NBS, we compared kinetic experiments of the inverse vulcanization of TMNBS, MENBS, DENBS, and TENBS with elemental sulfur (Figure S6). The products of the inverse vulcanizations of equal amounts of sulfur and TMNBS, MENBS, DENBS, and TENBS were examined for residual crystalline sulfur and C=C double bonds after 1, 2, 3, and 5 h, respectively. For all NBS, the conversion of C=C double bonds was complete after 2 h, as determined by ^{1}H NMR spectroscopy (Figure S7). After a reaction time of 5 h, no melting peaks of sulfur were detected in the thermograms of any poly(S-*r*-NBS) as determined via differential scanning calorimetry (DSC). Generally, the conversion of sulfur was faster for the non-polar TMNBS (1 h) than for the slightly polar TENBS (3 h), which is attributed to the lower solubility of TENBS in molten sulfur (Figure S8). It was concluded that the reactivity of the NBS was sufficiently similar to conduct the inverse vulcanization as ternary mixtures containing sulfur as a monomer, TMNBS as a comonomer, and a M, D, or T siloxane precursor as a termonomer. The product of the inverse vulcanization of sulfur and NBS_x, poly(S-*r*-NBS_x), was kept in a liquid state at 100 °C and was hydrolyzed with 20.0 equiv of HCl (pH 3) relative to the hydrolysable ethoxy group for 18 h. For the hydrolysis of the chloro-substituted poly(S-*r*-DCNBS) and poly(S-*r*-TCNBS), deionized water (pH 7) was used since the hydrolysis of chlorosilanes generates HCl. The crude poly(S-*r*-NBS_x) was heated in an oven at 80 °C for 5 days and in a vacuum oven at 40 °C overnight to quantitatively drive the polycondensation towards the formation of siloxane bonds. The resulting polymers of the general formula *branch*-poly(S-*r*-NBS_x) were precipitated in methanol to yield thick flakes that turned into grey granules after drying (Figure 1A, Figure S9). As recently was also described by Pyun, the precipitation helped to significantly decrease the content of low molar mass oligomers (Figure S10).[10] The heterogenic hydrolysis and polycondensation in molten poly(S-*r*-NBS_x) made long reaction times necessary but allowed us to keep the polymer synthesis a solvent free process, which is desirable to uphold the green chemistry principles of the inverse vulcanization (Figure S11). Polycondensations in different solvents were investigated, too,

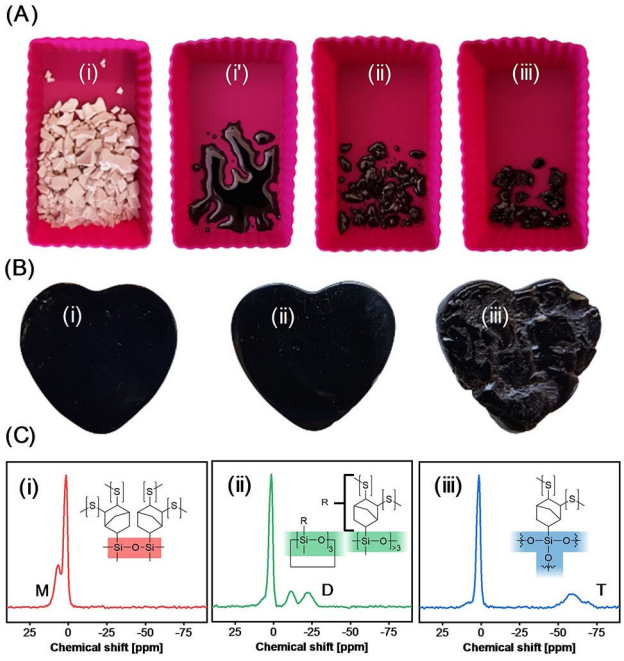

Figure 1. A) Melting behavior of *branch*-poly(S-*r*-NBS_{20}) with different degree of siloxane branching. Granules of *branch*-poly(S-*r*-$MENBS_{20}$) before (i) and after 2 h (i') at 80 °C. Granules of (ii) *branch*-poly(S-*r*-$DCNBS_{20}$) and (iii) *branch*-poly(S-*r*-$TCNBS_{20}$) after 2 h at 80 °C. B) Molded objects made from 2 g of *branch*-poly(S-*r*-NBS_{20}) at 80 °C overnight. While (i) *branch*-poly(S-*r*-$MENBS_{20}$) and (ii) *branch*-poly(S-*r*-$DCNBS_{20}$) adopted the shape of the mold, *branch*-poly(S-*r*-$TCNBS_{20}$) was still rubbery at 80 °C and did not fully adopt the shape of the mold. C) ^{29}Si CP/MAS NMR spectra of (i) *branch*-poly(S-*r*-$MENBS_{20}$), (ii) *branch*-poly(S-*r*-$DENBS_{20}$), and (iii) *branch*-poly(S-*r*-$TENBS_{20}$), showing characteristic peaks for M, D, and T siloxane bonds, respectively. The peak at 1.4 ppm present in each of the spectra corresponds to the trimethyl-substituted silicon atom stemming from the TMNBS comonomer.

but were ruled inferior to the heterogeneous melt polycondensation under practical and green chemistry aspects (Figure S12–15). Granulated *branch*-poly(S-*r*-$MENBS_{20}$) could be molded into different shapes by heating to 80 °C overnight (Figure 1B). Upon melting, the grey granules turned black, which is due to the reduction of light scattering. The polymer was homogeneous, which can be seen by the optical transparency of thin films (Figure S16). UV-vis spectroscopy of a film of *branch*-poly(S-*r*-$MENBS_{20}$) revealed that the black color stemmed from an absorption band spanning throughout the visible light spectrum (Figure S17). The molding behavior of *branch*-poly(S-*r*-$MENBS_{20}$), *branch*-poly(S-*r*-$DCNBS_{20}$), and *branch*-poly(S-*r*-$TCNBS_{20}$) differed drastically. After 2 hours at 80 °C, *branch*-poly(S-*r*-$MENBS_{20}$) spread as a viscous melt, *branch*-poly(S-*r*-$DCNBS_{20}$) formed droplets, and *branch*-poly(S-*r*-$TCNBS_{20}$) showed a color change from grey to black, due to the loss of surface porosity. The drastically different molding behavior is caused by the different type of siloxane bonding in the polymers.

To prove the presence of M, D, and T siloxane bonds in *branch*-poly(S-*r*-MENBS$_{20}$), *branch*-poly(S-*r*-DENBS$_{20}$), and *branch*-poly(S-*r*-TENBS$_{20}$) respectively, ^{29}Si cross polarization magic-angle spinning (CP MAS) NMR spectroscopy was used (Figure 1C). The MAS frequency was 12 kHz, and the CP contact time was 8 ms. Peaks at 1.4 ppm in all spectra correspond to the trimethyl-substituted silicon atom from TMNBS. The M siloxane bonds of *branch*-poly(S-*r*-MENBS$_{20}$) were confirmed by the peak found at 6.6 ppm.[21] For *branch*-poly(S-*r*-DENBS$_{20}$), two peaks at −11.4 and −22.2 ppm were observed, which correspond to short chains or cyclic siloxanes (MDM, D_3) and larger cyclic and linear oligomers ($MD_{>2}M$, $D_{>3}$), respectively.[21,22] The peaks found for *branch*-poly(S-*r*-TENBS$_{20}$) at −59.1 and −69.8 ppm are in the expected range for alkyl-substituted T siloxanes.[21,23] Due to the variety of possible chemical structures for T-siloxanes causing heterogeneous line-broadening in the spectrum of *branch*-poly(S-*r*-TENBS$_{20}$), the peaks were not assigned further.

To provide further evidence for the conversion of the hydrolysable ethoxy and chloro groups into siloxane bonds, we investigated *branch*-poly(S-*r*-NBS$_{20}$) polymers with infrared spectroscopy and compared the spectra to those of the respective monomers (Figure 2). The quantitative conversion of chloro substituents during the formation of *branch*-poly(S-*r*-DCNBS$_{20}$) and *branch*-poly(S-*r*-TCNBS$_{20}$) could be observed from the disappearance of the Si–Cl vibration bands at 537 cm^{-1} and 562 cm^{-1}, and from the appearance of a siloxane (Si–O–Si) band at 1136–956 cm^{-1} and 1164–956 cm^{-1}, respectively. In the ATR FT-IR spectrum of MENBS the strong doublet of the ethoxy group at 1107 and 1078 cm^{-1} disappeared and a siloxane band from 1092–999 cm^{-1} was observed in the spectrum of *branch*-poly(S-*r*-MENBS$_{20}$). The doublets in the spectrum of the ethoxy groups in DENBS at 1103 and 1074 cm^{-1} and in TENBS at 1101 and 1074 cm^{-1} transformed into siloxane bands from 1136–956 cm^{-1} in the spectrum of *branch*-poly(S-*r*-DENBS$_{20}$) and 1179–979 cm^{-1} in the spectrum of *branch*-poly(S-*r*-TENBS$_{20}$), respectively. Despite being derived from different hydrolysable groups (i.e., ethoxysilane and chlorosilane), the siloxane bonds in *branch*-poly(S-*r*-DENBS$_{20}$) and *branch*-poly(S-*r*-DCNBS$_{20}$), as well as *branch*-poly(S-*r*-TENBS$_{20}$) and *branch*-poly(S-*r*-TCNBS$_{20}$), were similar due to being D and T siloxanes, respectively. Based on a comparison with linear polydimethylsiloxane (PDMS), both *branch*-poly(S-*r*-DENBS$_{30}$) and *branch*-poly(S-*r*-DCNBS$_{30}$) polymers possessed nearly identical cyclic and linear siloxane binding motifs (Figure S18).

The underlying control mechanism for the inverse vulcanized polymers is the finely tunable increase of siloxane bonding between polymer chains. This allowed us to keep the elemental composition of all *branch*-poly(S-*r*-NBS$_x$) polymers essentially the same, as demonstrated by elemental analysis (Table 1). The *branch*-poly(S-*r*-NBS$_x$) polymers contained, on average, 36.1 ± 0.9 wt % C, 4.8 ± 0.6 wt % H, and 49.9 ± 1.1 wt % S, which is very close to the expected values assuming a quantitative formation of siloxane bonds. For example, for *branch*-poly(S-*r*-MENBS$_{10}$) a theoretical content of 35.7 wt % C, 5.4 wt % H, and 50.5 wt % S and for *branch*-poly(S-*r*-TENBS$_{20}$) 34.7 wt % C, 5.0 wt % H, and 52.3 wt % S was calculated. Thus, the *branch*-poly(S-*r*-NBS$_x$) polymers contain, on average, a minimum of 5.3 (*branch*-poly(S-*r*-MENBS$_{10}$) and a maximum of 5.6 sulfur atoms (*branch*-poly(S-*r*-TENBS$_{20}$) for every NBS unit.

The molar mass is arguably the most fundamental and relevant molecular property of polymers. While there are various strategies for carbon based polymers to control their molar mass, there are few systematic approaches for polymers prepared via inverse vulcanization.[10,19] The siloxane approach presented herein allows control over the weight average molar mass (M_W) via the relative amount and the type (i.e. M, D, T) of the siloxane precursor added. Six different *branch*-poly(S-*r*-MENBS$_x$) polymers with *x* being 10, 20, 30, 50, and 100 wt % were prepared and their

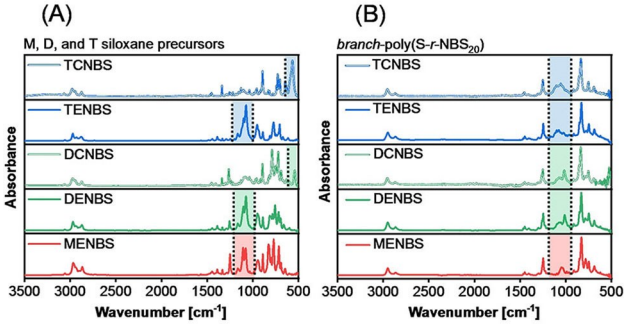

Figure 2. A) ATR FT-IR spectra of M, D, and T siloxane precursor termonomers. The dashed line highlights peaks corresponding to the hydrolysable ethoxy (MENBS, DENBS, TENBS) or chloro (DCNBS, TCNBS) groups. B) ATR FT-IR spectra of *branch*-poly(S-*r*-NBS$_{20}$) for different termonomers. The weight ratio of the termonomer relative to the TMNBS comonomer was 20 wt %. The dashed line highlights the area of characteristic siloxane vibrations.

Table 1: Elemental analysis of poly(S-*r*-TMNBS) and *branch*-poly(S-*r*-NBS$_x$) with varying contents of M, D, and T building blocks. Each value represents an average of two measurements which did not differ by more than 1 %.

Name	C (wt %)	H (wt %)	S (wt %)
poly(S-*r*-TMNBS)	38.8	5.6	48.6
branch-poly(S-*r*-MENBS$_{10}$)	35.9	4.9	51.1
branch-poly(S-*r*-MENBS$_{20}$)	35.2	4.9	50.6
branch-poly(S-*r*-MENBS$_{30}$)	35.1	4.7	52.0
branch-poly(S-*r*-MENBS$_{50}$)	34.9	4.6	49.9
branch-poly(S-*r*-DENBS$_{10}$)	36.3	3.7	50.5
branch-poly(S-*r*-DENBS$_{20}$)	35.6	3.7	49.7
branch-poly(S-*r*-DENBS$_{30}$)	35.3	4.0	49.7
branch-poly(S-*r*-DCNBS$_{10}$)	37.5	5.7	47.8
branch-poly(S-*r*-DCNBS$_{20}$)	37.7	5.7	48.4
branch-poly(S-*r*-DCNBS$_{30}$)	37.7	5.7	48.9
branch-poly(S-*r*-TENBS$_{10}$)	36.0	4.9	50.8
branch-poly(S-*r*-TENBS$_{20}$)	35.5	4.8	51.1
branch-poly(S-*r*-TCNBS$_{10}$)	36.8	5.2	49.1
branch-poly(S-*r*-TCNBS$_{20}$)	36.0	4.9	49.1

molar mass distribution was analyzed with GPC (Figure 3A). Poly(S-*r*-TMNBS$_{100}$), containing no MENBS, was used as a reference and treated the same as the MENBS containing polymers. It was found that the M_W increased with an increasing content of MENBS, whereas the M_N increased only slightly. This can be explained with the discriminating mechanism of polymer chain formation and was investigated with a chain distribution model (Figure S19–20). In brief, long polymer chains formed after the inverse vulcanization of an NBS$_x$ mixture have a higher chance to contain hydrolysable MENBS units than short ones. Only chains containing at least one MENBS unit can form siloxane bonds with each other, leading to a preferential growth of long chains. Notably, the obtained molar mass distributions of *branch*-poly(S-*r*-MENBS$_x$) polymers displayed fewer low molar mass species than those of other inverse vulcanization polymers such as poly(S-*r*-diisopropenylbenzene) or poly(S-*r*-styrene) (Figure S21). All *branch*-poly(S-*r*-MENBS$_x$) polymers with x being 0, 10, 20, 30, and 50 were soluble ($>100\ mg\,mL^{-1}$) in tetrahydrofuran, whereas the polycondensation of poly(S-*r*-MENBS$_{100}$) yielded the insoluble *net*-poly(S-*r*-MENBS$_{100}$).

The insolubility and brittleness of *net*-poly(S-*r*-MENBS$_{100}$) was attributed to the high degree of M siloxane crosslinking, which could be controlled via partial polycondensation, i.e., by using below stoichiometric amounts ($\ll 1.00$ equiv) of HCl (pH 3) relative to the hydrolysable ethoxy group. With an increasing amount of water, the partial polycondensation of poly(S-*r*-MENBS$_{100}$) yielded viscous, flexible, and brittle polymers, which unfortunately hardened and became brittle over the course of several weeks (Figure S22–S25). The embrittlement of partially hydrolyzed *net*-poly(S-*r*-MENBS$_{100}$) was attributed to air moisture, which slowly increased the degree of siloxane crosslinking via hydrolysis and polycondensation.

ATR FT-IR was used to prove that the increase of the MENBS content in the NBS$_x$ mixture led to a factual increase of M siloxane bonds in *branch*-poly(S-*r*-MENBS$_x$) polymers (Figure 3B). A comparison of the siloxane vibration bands between 1092 and 999 cm^{-1} revealed integral ratios of 1.95, 3.14, and 4.86 between *branch*-poly(S-*r*-MENBS$_{10}$) and *branch*-poly(S-*r*-MENBS$_{20}$), *branch*-poly(S-*r*-MENBS$_{30}$), and *branch*-poly(S-*r*-MENBS$_{50}$), respectively, which is close to the expected values 2, 3, and 5. A linear relation between the integrals and the concentrations of functional groups is only valid when the dipole moments of the vibrations are identical. Here, *branch*-poly(S-*r*-MENBS$_x$) with an increasing content of the same M–M siloxane bond were compared, thus a linear dependence can be assumed. It was concluded that the increase of MENBS in the feed ratio of the NBS$_x$ mixture leads to a proportional increase of M siloxane bonds in the *branch*-poly(S-*r*-MENBS$_x$) polymers.

To investigate the influence of the different siloxane bonds, i.e., M, D, and T siloxane bonds, as well as the influence of the hydrolysable functional group, i.e., ethoxy- and chloro, on the molar mass, we synthesized *branch*-poly(S-*r*-NBS$_{20}$) polymers using NBS$_x$ mixtures containing 20 wt % of MENBS, DENBS, DCNBS, TENBS, or TCNBS, and 80 wt % of TMNBS. GPC analysis of the *branch*-poly(S-*r*-NBS$_{20}$) revealed that the M_W increased from M, to D, to T siloxane bond containing polymers (Figure 3C). Polymers made from ethoxy-substituted DENBS yielded a higher molar mass than those prepared from the chloro-substituted DCNBS. This might be due a preferential formation of small cyclosiloxane rings resulting from the faster hydrolysis of chlorosilanes compared to ethoxysilanes. For *branch*-poly(S-*r*-DENBS$_{30}$) and *branch*-poly(S-*r*-DCNBS$_{30}$), however, no such effect was observed, and both had a very similar M_W (Table 2). The molar mass distribution of the T siloxane bond containing polymer *branch*-poly(S-*r*-TCNBS$_{20}$) split up into a bimodal molar mass distribution and had a far higher average M_W than *branch*-poly(S-*r*-TENBS$_{20}$). We attribute this to the lesser steric hindrance and higher reactivity of trichlorosilanes towards hydrolysis compared to triethoxysilanes, which could cause extreme local growth of the polymer due to the heterogeneity of the polycondensation. It can be ensured that the high molar mass distribution observed in the GPC traces of *branch*-poly(S-*r*-TCNBS$_{20}$) is not a homopolymer of polycondensated TCNBS, since aliphatic poly(siloxane)s do not absorb UV light (Figure S26). To detect the maximum molar mass of fully soluble *branch*-poly(S-*r*-NBS$_x$) polymers, we synthesized *branch*-poly(S-*r*-NBS$_x$) with varying contents of MENBS, DENBS, DCNBS, TENBS, and TCNBS, and determined their molar mass with GPC (Figure S27). As a general trend, the resulting M_W of all *branch*-poly(S-*r*-NBS$_x$) increased with

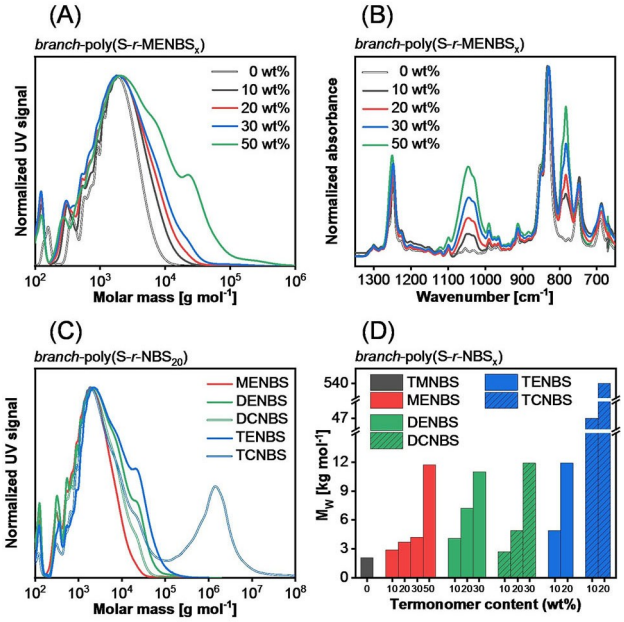

Figure 3. A) GPC traces and B) ATR FT-IR spectra of *branch*-poly(S-*r*-MENBS$_x$) with x being 10, 20, 30, and 50 wt %. The sample for x being 0 wt % is poly(S-*r*-TMNBS$_{100}$). C) GPC traces of *branch*-poly(S-*r*-NBS$_{20}$) with NBS being either MENBS, DENBS, DCNBS, TENBS, or TCNBS. The weight ratio of the respective, termonomer relative to TMNBS was 20 wt %. D) Comparison of the weight average molar mass (M_W) in dependence of the type and the amount of the termonomer.

Table 2: Average molar mass (M_N, M_W), $Đ$ and glass transition temperature (T_G) of *branch*-poly(S-*r*-NBS_x) with varying contents of M, D, and T building blocks.

Name	M_N [gmol^{-1}]	M_W [gmol^{-1}]	$Đ$	T_G [°C]
poly(S-*r*-TMNBS)	1100	2100	1.9	6
branch-poly(S-*r*-$MENBS_{10}$)	900	2900	3.2	10
branch-poly(S-*r*-$MENBS_{20}$)	900	3700	4.1	14
branch-poly(S-*r*-$MENBS_{30}$)	900	4200	4.7	18
branch-poly(S-*r*-$MENBS_{50}$)	1200	11 700	9.8	27
branch-poly(S-*r*-$DENBS_{10}$)	1100	4100	3.7	15
branch-poly(S-*r*-$DENBS_{20}$)	1100 ± 100	7600 ± 700[a]	6.5	26
branch-poly(S-*r*-$DENBS_{30}$)	1100	11 000	10.0	35
branch-poly(S-*r*-$DCNBS_{10}$)	900	2700	3.0	14
branch-poly(S-*r*-$DCNBS_{20}$)	1100	4900	4.5	23
branch-poly(S-*r*-$DCNBS_{30}$)	1100	11 900	10.1	35
branch-poly(S-*r*-$TENBS_{10}$)	1900	8600	4.5	17
branch-poly(S-*r*-$TENBS_{20}$)	1900	11 000	5.8	22
branch-poly(S-*r*-$TCNBS_{10}$)	800	47 000	59	11
branch-poly(S-*r*-$TCNBS_{20}$)	1400	54 0000	386	20

[a] Average and SD ($n = 3$).

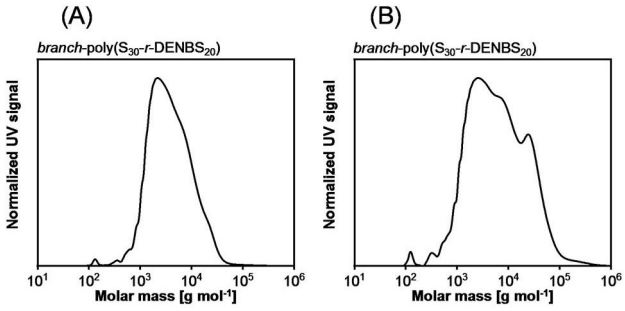

Figure 4. GPC traces of *branch*-poly(S_x-*r*-$DENBS_{20}$) with a sulfur content of A) 30 wt% ($M_N = 2400$, $M_W = 6000$) and B) 40 wt% ($M_N = 2700$, $M_W = 13900$). Elemental analysis of *branch*-poly(S_{30}-*r*-$DENBS_{20}$): 49.6 wt% C, 6.2 wt% H, and 32.7 wt% S. Elemental analysis of *branch*-poly(S_{40}-*r*-$DENBS_{20}$): 41.7 wt% C, 5.7 wt% H, and 41.4 wt% S.

increasing amount of the respective siloxane precursor (Figure 3D, Table 2). The M_N and M_W of independently prepared *branch*-poly(S-*r*-$DENBS_{20}$) polymers were 1100 ± 100 g mol^{-1} and 7600 ± 700 g mol^{-1}, respectively, indicating acceptable reproducibility (Figure S28). *Branch*-poly(S-*r*-$MENBS_x$) polymers derived from the inverse vulcanization and polycondensation of NBS_x mixtures exceeding either 50 wt% of MENBS, 30 wt% of DENBS or DCNBS, and 20 wt% of TENBS or TCNBS, were not fully soluble in tetrahydrofuran, dichloromethane, or chloroform. The chemical structure and the incorporation of increasing amounts of the M, D, and T siloxanes bonds in *branch*-poly(S-*r*-$MENBS_x$) polymers were confirmed with ATR FT-IR (Figure S29–S34). After a storage time of one month, all *branch*-poly(S-*r*-NBS_{20}) were free of crystalline elemental sulfur, as indicated by the absence of melting peaks in DSC curves, the absence of reflexes in pXRD patterns and the homogeneity of the elemental composition in EDX spectra (Figure S35–S37).

To investigate the influence of the sulfur content on the inverse vulcanization and polycondensation of NBS, *branch*-poly(S_x-*r*-$DENBS_{20}$) was chosen as a model system and the feed ratio of sulfur was varied from 30, 40, 50, 60, to 70 wt% of the total mass. Interestingly, for low amounts of sulfur, i.e., 30 and 40 wt%, narrow molar mass distributions that were free of low molar mass species were found (Figure 4). Consequently, the M_N of *branch*-poly(S_{30}-*r*-$DENBS_{20}$) and *branch*-poly(S_{40}-*r*-$DENBS_{20}$) were higher than for any other *branch*-poly(S-*r*-NBS_x) polymer ($M_N = 2400$ g mol^{-1}, $M_W = 6000$ g mol^{-1}, and $M_N = 2700$ g mol^{-1}, $M_W = 13900$ g mol^{-1}, respectively). Oppositely, for high amounts of sulfur (60 and 70 wt%) much more low molar mass species were found, and the average molar mass decreased (Figure S38). This might be explained by the ratio of sulfur atoms to NBS units of 2.5 and 3.7 for *branch*-poly(S_{30}-*r*-$DENBS_{20}$) and *branch*-poly(S_{40}-*r*-$DENBS_{20}$), respectively, which could facilitate the formation of stable disulfide, trisulfide, and tetrasulfide bridges between NBS units, rather than sulfur loops.

The type and amount of siloxane binding in *branch*-poly(S-*r*-NBS_x) was expected to influence the thermomechanical properties of the polymers. To investigate the thermomechanical properties of *branch*-poly(S-*r*-NBS_x), the glass transition temperature (T_G) of *branch*-poly(S-*r*-NBS_x) was determined via DSC for different contents of the M, D, or T precursor (Table 2, Figure S39–S41). With increasing content of the respective siloxane bonds, the T_G increased controllably. The T_G of *branch*-poly(S-*r*-$MENBS_x$) was 10, 14, 18, and 27 °C for x being 10, 20, 30, and 50 wt% of MENBS, respectively, whereas the T_G of poly(S-*r*-TMNBS) without siloxane bonds was 6 °C.

For *branch*-poly(S-*r*-$DENBS_x$) the T_G was 15, 26, and 35 °C for x being 10, 20, and 30 wt%, respectively, while for *branch*-poly(S-*r*-$DCNBS_x$) the T_G was 14, 23, and 35 °C for x being 10, 20, and 30 wt%, respectively. This was expected, since D siloxane bonds cause stronger branching of polymer chains than M siloxane bonds, resulting in a more restricted chain mobility and a higher T_G. However, the T_G did not increase further from D to T siloxane bond containing polymers as we anticipated. While the T_G of *branch*-poly(S-*r*-$TENBS_{10}$) was the highest amongst the *branch*-poly(S-*r*-NBS_{10}) polymers (17 °C), the T_Gs of *branch*-poly(S-*r*-$TENBS_{20}$), *branch*-poly(S-*r*-$TCNBS_{10}$), and *branch*-poly(S-*r*-$TCNBS_{20}$) were comparably low (22, 11, and 20 °C, respectively). Presumably, polymers branched by T siloxane bonds do not participate in the chain mobility at the determined T_Gs. To conclude, the T_G could be increased steadily by the content of M and D siloxane bonds in the polymers. Also, the T_G could be controlled by the type of siloxane bonds, as shown by an increase of the T_G from the M siloxane polymers *branch*-poly(S-*r*-$MENBS_x$) to the D siloxane polymers *branch*-poly(S-*r*-$DENBS_x$) and *branch*-poly(S-*r*-$DCNBS_x$). However, the T_G of T siloxane containing polymers was not indicative for their macroscopic viscous behavior.

To provide a more accurate examination of the thermomechanical properties of *branch*-poly(S-*r*-NBS_x) in depend-

ence of the type of siloxane, small amplitude oscillatory shear rheology was conducted using poly(S-*r*-MENBS$_{20}$), *branch*-poly(S-*r*-DCNBS$_{20}$), and *branch*-poly(S-*r*-TCNBS$_{20}$) containing M, D, and T siloxane bonds, respectively (Figure 5A). The choice of the type of siloxane in *branch*-poly(S-*r*-NBS$_x$) polymers allowed a controlled increase of the M_W, which has significant influence on the viscoelastic properties of polymers. Thus, the storage (G′) and loss moduli (G″) of poly(S-*r*-MENBS$_{20}$), *branch*-poly(S-*r*-DCNBS$_{20}$), and *branch*-poly(S-*r*-TCNBS$_{20}$) were determined for different temperatures. While *branch*-poly(S-*r*-MENBS$_{20}$) and *branch*-poly(S-*r*-DCNBS$_{20}$) were found to be in the flow regime (G″ > G′) at 40 and 60 °C, *branch*-poly(S-*r*-TCNBS$_{20}$) showed a cross over at 0.17 (60 °C), 6.5 (80 °C), and 74.5 rad s^{-1} (100 °C), before which elastic behavior (G″ > G′) dominated (Figure S42). At 120 °C, *branch*-poly(S-*r*-TCNBS$_{20}$) showed a dominant viscous behavior below 0.22 rad s^{-1} upon which the elastic behavior dominated until 100 rad s^{-1}. The storage and loss moduli at 1 rad s^{-1} and 60 °C were 0.3, 14.0, and 32.5 kPa (G′) and 1.0, 33.0, and 45.0 kPa (G″) for *branch*-poly(S-*r*-MENBS$_{20}$), *branch*-poly(S-*r*-DCNBS$_{20}$), and *branch*-poly(S-*r*-TCNBS$_{20}$), respectively. This significant difference is attributed to the type of siloxane binding in the polymers.

The complex viscosity of *branch*-poly(S-*r*-MENBS$_{20}$) melts were found to be independent of the frequency between 0.1 and 1 rad s^{-1}. Thus, a series of *branch*-poly(S-*r*-MENBS$_x$) with x being 15, 20, and 25 wt % was synthesized to investigate the influence of small compositional differences on the zero-shear viscosity η_0 (Figure 5B, Figure S43). The zero-shear viscosities were obtained as the average of the complex viscosity between 0.1 and 1 rad s^{-1} and its standard deviation, i.e., 622 ± 15, 1053 ± 29, 3027 ± 10 Pas at 60 °C and 28.500 ± 1100, 63.800 ± 1900, and 149 000 ± 12 200 Pas at 40 °C for *branch*-poly(S-*r*-MENBS$_{15}$), *branch*-poly(S-*r*-MENBS$_{20}$), and *branch*-poly(S-*r*-MENBS$_{25}$), respectively. Thus, the zero-shear viscosities increased with increasing content of siloxane bonds.

Consequently, *branch*-poly(S-*r*-MENBS$_{15}$) creeped faster than *branch*-poly(S-*r*-MENBS$_{20}$), or *branch*-poly(S-*r*-MENBS$_{25}$). The zero-shear viscosities of *branch*-poly(S-*r*-MENBS$_{15}$), *branch*-poly(S-*r*-MENBS$_{20}$), and *branch*-poly(S-*r*-MENBS$_{25}$) were within and above the range of PDMS oils (ca. 0.001–2000 Pas).[24]

To test whether small changes in the MENBS content of *branch*-poly(S-*r*-NBS$_x$) polymers would influence their viscoelastic properties, we performed tensile tests with *branch*-poly(S-*r*-MENBS$_{15}$), *branch*-poly(S-*r*-MENBS$_{20}$), and *branch*-poly(S-*r*-MENBS$_{25}$) polymers (Figure S44). All three polymers were able to maintain more than 1000 % strain without breaking as expected from the viscoelastic liquid-like behavior observed from rheology measurements and due to the room temperature of 28 °C during the measurements being 15 °C above the T_G of *branch*-poly(S-*r*-MENBS$_{20}$). The maximum stress required to deform the polymers increased with the MENBS content and was 122 ± 3 kPa for *branch*-poly(S-*r*-MENBS$_{15}$) 265 ± 84 kPa for *branch*-poly(S-*r*-MENBS$_{20}$), and 418 ± 55 kPa for *branch*-poly(S-*r*-MENBS$_{25}$). The toughness of *branch*-poly(S-*r*-MENBS$_x$) was also enhanced with the MENBS content (Figure S45), which was determined to be 0.40 ± 0.06 MJ m^{-3} for *branch*-poly(S-*r*-MENBS$_{15}$), 1.41 ± 0.48 MJ m^{-3} for *branch*-poly(S-*r*-MENBS$_{20}$), and 1.97 ± 0.37 MJ m^{-3} for *branch*-poly(S-*r*-MENBS$_{25}$).

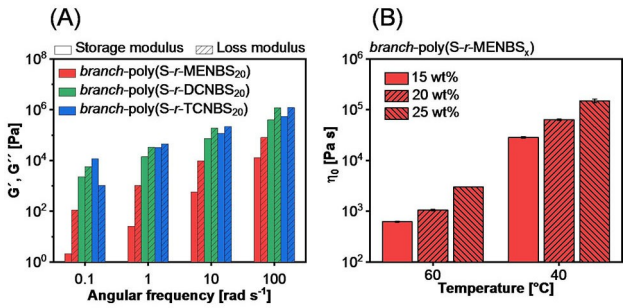

Figure 5. Investigation of thermomechanical properties with small amplitude oscillatory shear rheology. A) Comparison of the storage and loss moduli for *branch*-poly(S-*r*-NBS$_{20}$) at 60 °C with NBS being either MENBS, DCNBS, or TCNBS. B) Comparison of the zero-shear viscosity η_0 of *branch*-poly(S-*r*-MENBS$_x$) at 40 and 60 °C for *x* being 15, 20, and 25 wt %.

Conclusion

The inverse vulcanization of chloro- and ethoxynorbornenylsilanes has been reported for the first time which demonstrated the compatibility of hydrolysable silanes with the harsh conditions of the inverse vulcanization. Ethoxy- and chlorosilanes used as termonomers were shown to strongly influence the properties of high sulfur content polymers by installing covalent M, D, or T siloxane bonds between polymer chains. Both the type and the amount of siloxane bonds could alter the properties of polymers significantly, whereas the amount of sulfur could be kept high (ca. 50 wt %) and constant. Hydrolysable vinylsilanes could be generally used to alter the properties of products of inverse vulcanizations that allow their presence as termonomer, which applies to most monomers reported for the inverse vulcanization. The siloxane-based approach herein is not the first strategy based on post-crosslinking of inverse vulcanization polymers. However, it is the first to comprehensively and systematically explore the branching of high sulfur content polymers below the threshold of crosslinking and insolubility. The combination of M, D, and T siloxane binding motifs within the same polymer has not been exploited yet and is subject to future research. Purification by precipitation resulted in the near quantitative removal of low molar mass species for *branch*-poly(S$_{30}$-*r*-DENBS$_{20}$) and *branch*-poly(S$_{40}$-*r*-DENBS$_{20}$), which are examples for purely unimodal and bimodal distributions for inverse vulcanized polymers with a sulfur content of 30 and 40 wt %, respectively, which is an important step towards model polymers with a narrow molar mass distribution. Spontaneous siloxane bonding of poly(S-*r*-NBS$_x$) triggered by air moisture at room temperature, as

observed for poly(S-*r*-MENBS$_{100}$) and poly(S-*r*-DENBS$_{100}$), could be very interesting for applications as glues and adhesives.

Acknowledgements

This project was partly supported by DFG (Heisenbergprofessur Projektnummer: 406232485, LE 2936/9-1). This work was funded by the Deutsche Forschungsgemeinschaft (DFG, German Research Foundation) under Germany's Excellence Strategy 2082/1-390761711 (Excellence Cluster "3D Matter Made to Order"). J. M. S. and P. F. thank the Deutsche Bundesstiftung Umwelt (DBU) for financial support. Timo Sehn is thanked for help with DSC analysis. Open Access funding enabled and organized by Projekt DEAL.

Conflict of Interest

The authors declare no conflict of interest.

Data Availability Statement

The data that support the findings of this study are available in the Supporting Information of this article.

Keywords: Inverse Vulcanization · Molar Mass · Norbornenyl Silanes · Siloxane

[1] W. J. Chung, J. J. Griebel, E. T. Kim, H. Yoon, A. G. Simmonds, H. J. Ji, P. T. Dirlam, R. S. Glass, J. J. Wie, N. A. Nguyen et al., *Nat. Chem.* **2013**, *5*, 518.

[2] a) M. J. H. Worthington, R. L. Kucera, I. S. Albuquerque, C. T. Gibson, A. Sibley, A. D. Slattery, J. A. Campbell, S. F. K. Alboaiji, K. A. Muller, J. Young et al., *Chem. Eur. J.* **2017**, *23*, 16219; b) M. P. Crockett, A. M. Evans, M. J. H. Worthington, I. S. Albuquerque, A. D. Slattery, C. T. Gibson, J. A. Campbell, D. A. Lewis, G. J. L. Bernardes, J. M. Chalker, *Angew. Chem. Int. Ed.* **2016**, *55*, 1714; *Angew. Chem.* **2016**, *128*, 1746; c) M. Thielke, L. Bultema, D. Brauer, B. Richter, M. Fischer, P. Theato, *Polymer* **2016**, *8*, 266; d) N. A. Lundquist, M. J. Sweetman, K. R. Scroggie, M. J. H. Worthington, L. J. Esdaile, S. F. K. Alboaiji, S. E. Plush, J. D. Hayball, J. M. Chalker, *ACS Sustainable Chem. Eng.* **2019**, *7*, 11044; e) D. J. Parker, H. A. Jones, S. Petcher, L. Cervini, J. M. Griffin, R. Akhtar, T. Hasell, *J. Mater. Chem. A* **2017**, *5*, 11682; f) M. J. H. Worthington, C. J. Shearer, L. J. Esdaile, J. A. Campbell, C. T. Gibson, S. K. Legg, Y. Yin, N. A. Lundquist, J. R. Gascooke, I. S. Albuquerque et al., *Adv. Sustainable Syst.* **2018**, *2*, 1800024; g) L.-A. Ko, Y.-S. Huang, Y. A. Lin, *ACS Appl. Polym. Mater.* **2021**, *3*, 3363.

[3] a) Z. Deng, A. Hoefling, P. Théato, K. Lienkamp, *Macromol. Chem. Phys.* **2018**, *219*, 1700497; b) J. A. Smith, R. Mulhall, S. Goodman, G. Fleming, H. Allison, R. Raval, T. Hasell, *ACS Omega* **2020**, *5*, 5229.

[4] C. Herrera, K. J. Ysinga, C. L. Jenkins, *ACS Appl. Mater. Interfaces* **2019**, *11*, 35312.

[5] a) Y. Xin, H. Peng, J. Xu, J. Zhang, *Adv. Funct. Mater.* **2019**, *29*, 1808989; b) T. R. Martin, K. A. Mazzio, H. W. Hillhouse, C. K. Luscombe, *Chem. Commun.* **2015**, *51*, 11244.

[6] a) J. J. Griebel, S. Namnabat, E. T. Kim, R. Himmelhuber, D. H. Moronta, W. J. Chung, A. G. Simmonds, K.-J. Kim, J. van der Laan, N. A. Nguyen et al., *Adv. Mater.* **2014**, *26*, 3014; b) J. J. Griebel, N. A. Nguyen, S. Namnabat, L. E. Anderson, R. S. Glass, R. A. Norwood, M. E. Mackay, K. Char, J. Pyun, *ACS Macro Lett.* **2015**, *4*, 862; c) T. S. Kleine, L. R. Diaz, K. M. Konopka, L. E. Anderson, N. G. Pavlopolous, N. P. Lyons, E. T. Kim, Y. Kim, R. S. Glass, K. Char et al., *ACS Macro Lett.* **2018**, *7*, 875; d) T. S. Kleine, T. Lee, K. J. Carothers, M. O. Hamilton, L. E. Anderson, L. Ruiz Diaz, N. P. Lyons, K. R. Coasey, W. O. Parker, L. Borghi et al., *Angew. Chem. Int. Ed.* **2019**, *58*, 17656–17660; *Angew. Chem.* **2019**, *131*, 17820–17824; e) D. A. Boyd, V. Q. Nguyen, C. C. McClain, F. H. Kung, C. C. Baker, J. D. Myers, M. P. Hunt, W. Kim, J. S. Sanghera, *ACS Macro Lett.* **2019**, *8*, 113; f) D. A. Boyd, C. C. Baker, J. D. Myers, V. Q. Nguyen, G. A. Drake, C. C. McClain, F. H. Kung, S. R. Bowman, W. Kim, J. S. Sanghera, *Chem. Commun.* **2017**, *53*, 259.

[7] a) I. Gomez, O. Leonet, J. A. Blazquez, D. Mecerreyes, *ChemSusChem* **2016**, *9*, 3419; b) Y. Zhang, J. J. Griebel, P. T. Dirlam, N. A. Nguyen, R. S. Glass, M. E. Mackay, K. Char, J. Pyun, *J. Polym. Sci. Part A* **2017**, *55*, 107; c) H. Kang, M. J. Park, *Nano Energy* **2021**, *89*, 106459; d) L. Zhang, L. Ge, G. He, Z. Tian, J. Huang, J. Wang, D. J. Brett, J. Hofkens, F. Lai, T. Liu, *J. Phys. Chem. C* **2021**, *125*, 18604; e) T. Zhang, F. Hu, W. Shao, S. Liu, H. Peng, Z. Song, C. Song, N. Li, X. Jian, *ACS Nano* **2021**, *15*, 15027–15038.

[8] a) N. A. Lundquist, A. D. Tikoalu, M. J. H. Worthington, R. Shapter, S. J. Tonkin, F. Stojcevski, M. Mann, C. T. Gibson, J. R. Gascooke, A. Karton et al., *Chem. Eur. J.* **2020**, *26*, 10035; b) S. J. Tonkin, C. T. Gibson, J. A. Campbell, D. A. Lewis, A. Karton, T. Hasell, J. M. Chalker, *Chem. Sci.* **2020**, *11*, 5537–5546.

[9] a) A. M. Abraham, S. V. Kumar, S. M. Alhassan, *Chem. Eng. J.* **2018**, *332*, 1–7; b) M. S. Karunarathna, M. K. Lauer, T. Thiounn, R. C. Smith, A. G. Tennyson, *J. Mater. Chem. A* **2019**, *7*, 15683.

[10] K.-S. Kang, A. Phan, C. Olikagu, T. Lee, D. A. Loy, M. Kwon, H.-J. Paik, S. J. Hong, J. Bang, W. O. Parker et al., *Angew. Chem. Int. Ed.* **2021**, *60*, 22900–22907; *Angew. Chem.* **2021**, *133*, 23082–23089.

[11] I. Bu Najmah, N. A. Lundquist, M. K. Stanfield, F. Stojcevski, J. A. Campbell, L. J. Esdaile, C. T. Gibson, D. A. Lewis, L. C. Henderson, T. Hasell et al., *ChemSusChem* **2021**, *14*, 2352.

[12] a) M. Mann, J. E. Kruger, F. Andari, J. McErlean, J. R. Gascooke, J. A. Smith, M. J. H. Worthington, C. C. C. McKinley, J. A. Campbell, D. A. Lewis et al., *Org. Biomol. Chem.* **2019**, *17*, 1929; b) S. F. Valle, A. S. Giroto, R. Klaic, G. G. Guimarães, C. Ribeiro, *Polym. Degrad. Stab.* **2019**, *162*, 102.

[13] V. Gold, *The IUPAC Compendium of Chemical Terminology*, International Union of Pure and Applied Chemistry (IUPAC), Research Triangle Park, NC, **2019**.

[14] a) J. M. Chalker, M. J. H. Worthington, N. A. Lundquist, L. J. Esdaile, *Top. Curr. Chem.* **2019**, *377*, 16; b) Y. Zhang, R. S. Glass, K. Char, J. Pyun, *Polym. Chem.* **2019**, *10*, 4078.

[15] a) L. J. Dodd, Ö. Omar, X. Wu, T. Hasell, *ACS Catal.* **2021**, *11*, 4441; b) X. Wu, J. A. Smith, S. Petcher, B. Zhang, D. J. Parker, J. M. Griffin, T. Hasell, *Nat. Commun.* **2019**, *10*, 647; c) Y. Zhang, N. G. Pavlopoulos, T. S. Kleine, M. Karayilan, R. S. Glass, K. Char, J. Pyun, *J. Polym. Sci. Part A* **2019**, *57*, 7–12.

[16] K. Orme, A. H. Fistrovich, C. L. Jenkins, *Macromolecules* **2020**, *53*, 9353.

[17] a) J. A. Smith, S. J. Green, S. Petcher, D. J. Parker, B. Zhang, M. J. H. Worthington, X. Wu, C. A. Kelly, T. Baker, C. T.

Gibson et al., *Chem. Eur. J.* **2019**, *25*, 10433; b) B. Zhang, S. Petcher, T. Hasell, *Chem. Commun.* **2019**, *55*, 10681.
[18] J. A. Smith, X. Wu, N. G. Berry, T. Hasell, *J. Polym. Sci. Part A* **2018**, *56*, 1777.
[19] P. Yan, W. Zhao, B. Zhang, L. Jiang, S. Petcher, J. A. Smith, D. J. Parker, A. I. Cooper, J. Lei, T. Hasell, *Angew. Chem. Int. Ed.* **2020**, *59*, 13371–13378; *Angew. Chem.* **2020**, *132*, 13473–13480.
[20] J. M. Scheiger, C. Direksilp, P. Falkenstein, A. Welle, M. König-Edel, S. Heissler, J. Matysik, P. Levkin, P. Theato, *Angew. Chem. Int. Ed.* **2020**, *59*, 18639–18645; *Angew. Chem.* **2020**, *132*, 18798–18804.
[21] J. Sanchez, S. E. Rankin, A. V. McCormick, *Ind. Eng. Chem. Res.* **1996**, *35*, 117.
[22] Y. Sugahara, S. Okada, S. Sato, K. Kuroda, C. Kato, *J. Non-Cryst. Solids* **1994**, *167*, 21.
[23] Y. Sugahara, S. Okada, K. Kuroda, C. Kato, *J. Non-Cryst. Solids* **1992**, *139*, 25.
[24] a) M. Venczel, G. Bognár, Á. Veress, *Processes* **2021**, *9*, 331; b) Z. Kőkuti, K. van Gruijthuijsen, M. Jenei, G. Tóth-Molnár, A. Czirják, J. Kokavecz, P. Ailer, L. Palkovics, A. C. Völker, G. Szabó, *Appl. Rheol.* **2014**, *24*, 63984.

Manuscript received: November 3, 2021
Accepted manuscript online: January 24, 2022
Version of record online: ■■, ■■

Research Articles

Polymerization

J. M. Scheiger, M. Hoffmann, P. Falkenstein, Z. Wang, M. Rutschmann, V. W. Scheiger, A. Grimm, K. Urbschat, T. Sengpiel, J. Matysik, M. Wilhelm, P. A. Levkin,* P. Theato* e202114896

Inverse Vulcanization of Norbornenylsilanes: Soluble Polymers with Controllable Molecular Properties via Siloxane Bonds

Inverse vulcanized polymers of norbornenylsilanes with hydrolysable chloro- and ethoxy substituents were prepared and polycondensated to install defined amounts of M, D, or T siloxane bonds. The M_W and T_G of the soluble and branched polymers containing 50 wt% S could be varied systematically, whereas the elemental composition remained the same. Polymers with a sulfur content of 30 wt% could be prepared without low molar mass impurities.